Capillary Biochip for point of use biomedical application

Joana de Carvalho Rodrigues Mesquita Chim

Thesis to obtain the Master of Science Degree in

Biomedical Engineering

Supervisors: Prof. João Pedro Estrela Rodrigues Conde and Dr. João Garcia da Fonseca

Examination Committee

Chairperson: Prof. Raúl Daniel Lavado Carneiro Martins
Members of the Committee: Dr. Nuno Alexandre Esteves Reis
Prof. Frederico Castelo Alves Ferreira

October 2015

Abstract

Microfluidic devices have become an attractive technology in terms of point of care use, due to reduction of sample and reagents consumption, time and also costs of analysis. These devices allow to simplify laboratory protocols and perform them in a single chip of small dimensions. However, some of the devices developed require combining the chip with external equipment that can be complex for handling and difficult the PoC application.

In order to solve these issues, capillary chips come into play. Capillary-driven microfluidics introduce a wide range of benefits, including being user friendly and portability, owed to the fact that fluid flow is only controlled by the surface wetting properties of the device. Taking advantage of these benefits this work proposes a capillary chip for a specific biomedical application, namely an immunoassay or the detection of the mycotoxin OTA.

PDMS and glass were the materials chosen for the fabrication of the capillary chips. In addition an intensive study of the work conditions is presented. Namely the effect that different capillary pumps can have in fluid motion. Since surface properties are determinant in capillarity, the influence of the UV/Ozone treatment was also tested. In terms of application, the chip was shown to be capable of providing the required conditions for performing the OTA immunoassay. Demonstrating to be sensitive enough to allow the detection of OTA concentrations within the regulatory limits.

The capillary chip proposed in this project combines the requirements for a PoC device, easy to use and portable.

Key words: capillarity; microfluidic devices; capillary pumps; surface treatment; OTA immunoassay

1 INTRODUCTION

The conceptual idea behind microfluidic devices is that fluids can be manipulated in microscale devices, commonly known as miniaturized total analysis systems (μTASs). These systems introduced a wide variety of applications, from biology research to complex assay protocols and benefited from the significant reduction of sample volume, which in turn led to a decrease in cost of reagents and also provided the user with more control over the spatio-temporal dynamics of the assays conditions.[1]

A recent report from MarketsandMarkets refers that the evaluation of the microfluidic market for 2015 reaches the 3.1 billion dollars, and a forecast for 2020 sets a target of 7.5 billion dollars. Some of the major players include Agilent Technologies, Bio-Rad Laboratories,

Abbott Laboratories and Illumina.[2],[3] Another good indicator for the appeal of this area is the increasing number of spin-off companies that emerged, trying to commercialize lab on a chip (LoC) microfluidic products.[1]

In terms of the capillary driven tests or "lateral flow assays", the development started in the 1960s with a huge level of commercialization. Some examples of these products are the pregnancy and diabetes tests. The working principle is based in a passive liquid transport by capillary action within microchannels. These devices can be very appealing due to the possibility of performing on-site measurements in disposable and low cost devices.[1]

Capillary chips introduce a wide range of benefits, for instances the independence of external fluidic equipment that lead to portability and produce a short time analysis. Another advantage of these devices is the small user intervention, only related with loading of solutions at the inlet of the structure. Capillary flow is controlled by surface-liquid adhesion and liquid-liquid cohesion. This way, the flow depends on surface properties and geometry.[4] Several capillary components (e.g. valves and pumps) can be incorporated into the device to manipulate the fluid flow.[5]

Immunoassay experiments have been performed for a long time for a variety of applications, medical diagnostics, pharmaceutical, food safety and environmental analysis among others. Portable devices for immunodiagnostics are interesting for healthcare due to the possibility of decentralized and point of care testing.[6] These devices assemble a set of properties that make them attractive for diagnostic applications. The necessary sample volume is small and the devices can be portable, low cost, easy to use and require lower power consumptions. Test results can be acquired rapidly after introducing the sample. Also, since manual handling is minimal, errors and risk of contamination can be easily avoided resulting in a higher level of reproducibility.[5],[7]

In the end this work proposes an autonomous capillary PDMS-glass device for general biomedical applications. In order to demonstrate its performance several tests were made, including a specific OTA immunoassay. This allows to show that by customizing the chip is possible to produce a PoC device for specific applications. The capillary chip developed only requires manipulation in the insertion of solutions and signal reading and analysis.

1.1 Fluid Dynamics

When designing and fabricating microfluidic devices is important to understand the physical phenomena that are relevant in small length scales. Since the dimension of the objects will determine the forces that dominate. In microfluidics phenomena like surface tension, contact angle and hydraulic resistance are predominant.[8]

1.1.1 Surface Tension and contact angle

A molecule in the middle of a liquid is considered stable since it benefits from cohesive interactions with all its neighbors. However a molecule exposed on the surface doesn't have neighboring molecules in all directions, leading to an unbalanced net force. This way the molecules are pulled to the interior of the droplet creating an internal pressure. The result of the unbalanced forces will be the contraction of the liquid in order to achieve the lowest surface free energy. The intermolecular force responsible for contracting the surface is called surface tension.[9]

The contact angle represents a relative measure of the interfacial energy of the surfaces that are in contact. This parameter can be acquired by applying a tangent line from the point where the three phases liquid/solid/gas co-exist along the liquid-gas interface.[9] Contact angle has a close connection with surface tension that can be described by (equation1),

$$\cos\theta = \frac{\gamma_{sg} - \gamma_{sl}}{\gamma_{lg}} \qquad (1)$$

The wettability of a surface to a specific liquid, can be evaluated according with the angle produced, in fact a certain surface can be defined as wettable (or hydrophilic) if $\theta < 90°$ and non-wettable (or hydrophobic) when

$\theta > 90°$, where the liquid spreads or adopts a droplet form, respectively. For a solid-liquid system the contact angle is characteristic in specific environmental conditions.[10]

1.1.2 Capillary pressure

Capillary action results from the surface tension phenomenon. In this case, the liquid has the ability to flow due to the wetting properties of the surfaces that constitute the walls of the channel. In a microchannel with a rectangular cross section (w × d), fluid motion is pressure driven[11] and capillary forces depend on the contact angles of the liquid to each wall of the channel,[10]

$$\Delta p_s = \gamma \left(\frac{cos\theta_b + cos\theta_t}{d} + \frac{cos\theta_l + cos\theta_r}{w} \right) \quad (2)$$

In microchannels due to the characteristic small dimensions the Reynolds number is very low ($Re \ll 1$) and the flow is considered laminar. In this case inertial effects like gravity and turbulence can be neglected.[12]

These assumptions allow to simplify the Navier-Stokes, assuming a steady-state flow and that the channels are characterized by h ≪ w, is then possibly to obtain

$$Q = \frac{h^3 w}{12 \mu L} \Delta p \quad (3)$$

where Q represents the flow rate.[11] By analogy with a electrical circuit Q corresponds to electrical current, the pressure would represent the voltage. Consequently, allowing the definition of the hydraulic resistance. [13]

$$R(x) = R_{Hyd} = \frac{12 \mu L}{h^3 w} \quad (4)$$

In a capillary systems, the fluid motion is produced by a difference of pressure created by the properties of the surfaces that constitute the channel. The hydraulic resistance is accumulated as the fluid fills the structure, resulting in a decrease in flow rate.

1.1.3 Capillary pumps

Autonomous capillary systems are widely used for manipulating fluids for applications such as immunoassays and diagnostic applications. Let us consider the use of capillary pumps that determine the overall flow rate and volume of liquids that can be handled by the device. These structures can have diverse designs that will behave differently while controlling the advancement of the filling front.

The simplest design is a microchannel with the adequate volume to accommodate all the liquid. A more advanced pump can also be composed of elongated microstructures (posts) that control the filling front by imposing different times for the progression of the liquid along all the directions of the pump. These two different designs correspond to a *slow* and a *fast* pump.[14] In the *slow* pump, the accumulation of resistance leads to a decrease in flow rate. Whereas in the *fast* pump, the *passageways* created by the posts allow the fluid to pass, leading to an increase in fluid velocity. (As illustrated in Figure 1.1)

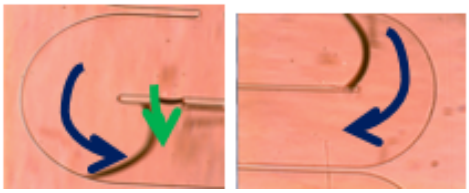

Figure 1.1 Illustration of the fluid flow through a *fast* (left) and a *slow* (right) pump

In terms of application the pumps can be used for specific steps of an assay, according with their characteristics. Namely, a *slow* pump is more adequate in steps for adsorption of molecules in the channel, or binding of antibodies and antigens, that require a slow velocity. On other hand a *fast* pump can be designed for washing steps. Therefore, is possible to tailor a capillary chip based in capillary pumps for a specific application, like an immunoassay.

1.1.4 PDMS-glass capillary device

PDMS is the most used polymer for the production of microfluidic flow paths. The widespread use of this polymer is related with the combination of material properties such as biocompatibility due to low toxicity, high electrical resistance, long-term endurance, low elastic modulus and flexible processing techniques.[15] However the use of this polymer shows some drawbacks like the possibility of nonspecific adsorption and permeation by

hydrophobic molecules, and poor wettability with aqueous solutions.[7],[16]

One way of addressing this challenge is to bond the hydrophobic structure to a hydrophilic material. Glass is characterized by a contact angle between 0 and 30º depending on the surface treatment, thus represents the hydrophilic substrate.[13]

$$\Delta p_s = \gamma \left(\frac{cos\theta_{glass} + cos\theta_{PDMS}}{d} + \frac{2cos\theta_{PDMS}}{w} \right) \quad (5)$$

As the equation suggests the wettable wall has a major impact in generating a positive capillary pressure to force the fluid motion within the channel. Therefore glass, that has a highly hydrophilic surface, can be chosen as the "motor" of the capillarity of this device.[17]

In order to achieve a functional PDMS-glass sealed microfluidic device it is essential to have both surfaces in contact, cleaned.

Surface tension and contact angle of a material depend on the formation of organic compounds. When the surface is contaminated the surface tension decreases and the contact angle is wider. Therefore is important to include a surface treatment step, to assure the proper conditions for capillary fluid motion.

UV/Ozone is the treatment considered in this work, that allows to remove the contaminants and also an increase in surface energy, that results in an enhance of hydrophilic and wettability behavior. [18]

1.1.5 OTA immunoassay

Ochratoxin A (OTA) is a mycotoxin involved in contamination of a variety of food (wine, beer and coffee) and feed at a global scale.[19]

European Union regulation has restricted limits to the concentration of this toxin in commercialized products.[20] Due to all the harmful effects related with this toxin, methods for the detection and quantification have been studied for a long time. Microfluidic devices are a good platform for the detection of this toxin, since they are not very time and reagent consuming.[21] This work proposes a capillary microfluidic device for the detection of this toxin.

2 METHODS

2.1 Capillary device fabrication

The first step to create the desired structure is the mask design in AUTOCAD. After creating the drawing, it is necessary to transfer it to an Aluminum substrate, obtained by depositing 2000 Å in a glass slide (Nordiko 7000). Then optical lithography is performed with a direct write laser that scans the surface and allows for the patterning of the AUTOCAD design.[22]

Once the hard mask is ready, the SU-8mold is fabricated. In order to obtain channels of 50µm height SU-8 50 is used, in a protocol [23],[24] that comprises the step of spin coating, soft bake and UV exposure for pattern definition, post exposure bake, development and at last hard bake. The profile of the channels on the SU-8 mold can be verified using a microscope and profilometer.

Afterwards is the PDMS fabrication. PDMS is obtained by mixing a curing agent with a liquid polymer base, and cure the mixture for 1:30h at 70ºC.[25]

At last the PDMS is peeled off from the mold and sealed with a glass slide that was subjected to wet cleaning with a detergent (Alconox) and to UV/Ozone treatment for 6min (UVO Cleaner 144AX-220, Jelight Company).

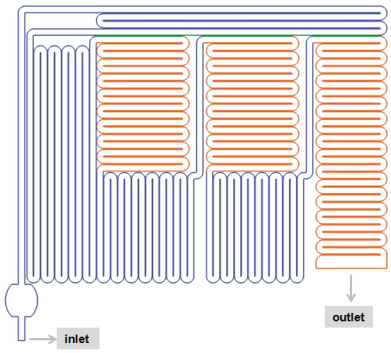

Figure 2.1 Illustration of the device structure used for performing the OTA immunoassays

The device structure is illustrated in Figure 2.1. This device is composed of a reaction

chamber, for signal reading, and for a sequence of *slow* and *fast* pumps.

2.2 Biological experiments

The OTA immunoassay (demonstranted in Figure 2.2) begins with the spotting of the OTA-BSA conjugate in the reaction chamber in the PDMS structure. After spotting the surface needs to be blocked (BSA) in order to avoid non-specific adsorption. Once the blocking is done, the remaining and not immobilized molecules have to be washed away. The washing step is executed by PBS.

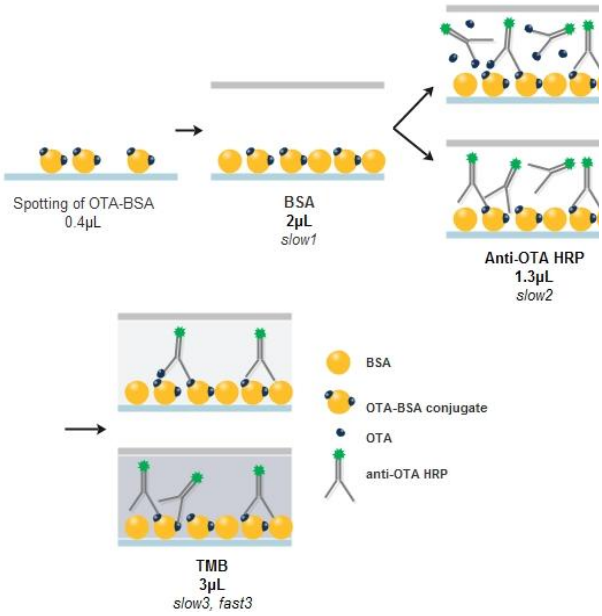

Figure 2.2 Schematics of the icELISA protocol.

After washing, the following solution introduced is anti-OTA HRP spiked with OTA at different concentrations, followed by another washing step. Finally the last solution introduced is TMB.

The introduction of all solutions is made manually, by approaching the pipette tip to the inlet near the reaction chamber. After passing through the entire device the liquid gets to the outlet. At this point no more liquid can enter the chip or be pumped, since all the pumps are full. The normal assay time is 15 minutes.

Besides studying the OTA immunoassay in PBS it was also included an immunoassay where the OTA was obtained from corn for salmon feed extracts (corn for salmon feed production kindly supplied by EWOS, Norway, within the framework of the FP7-SME EU DEMOTOX project - project reference 604752).

2.2.1 Data analysis

After the immunoassays the colorimetry is detected by optical microscopy. TMB flows in the final step of the assay and by reacting with HRP produces a colored product. The intensity of the signal is proportional to the amount of HRP present, which in turn is inversely proportional to the concentration of OTA tested. The produced signal is acquired by a camera connected to the optical microscope (Amscope). The analysis of the intensities obtained for different OTA concentrations is performed in the software ImageJ.

Since considering a colorimetric detection the results can be studied by calculating the light absorbance. The sample is excited by a light source and the regions of interest selected, namely for the background and for a spotted area. The mean intensities are obtained for these regions and the transmittance (T) is calculated. The relation between transmittance and absorbance is given by Beer-Lambert law,[26]

$$A = -\log(T) = -\log\left(\frac{\mathrm{I}}{\mathrm{I}_0}\right) \qquad (6)$$

For analysis the absorbance can then be plotted in function of the OTA concentration tested. It is important to include in this study the existing error for each measurement. The error bars used were obtained from the standard deviation of the data.[27]

3 RESULTS AND DISCUSSION

3.1 Optimization of capillary conditions

In order to have a working capillary system it is really essential to assure the right surface conditions, in terms of cleanness and surface treatment. Taking this into account, a significant amount of experiments performed in the capillary structures, with a diluted food dye, allowed to understand that there are critical conditions that need to be addressed.

The microscopic images presented in this work were acquired in an Olympus CKX-41 microscope (coupled with a digital camera Olympus XC30) and AmScope (coupled with a digital camera AmScope MD600) for the dye experiments and immunoassays, respectively.

3.1.1 Slow and fast pumps

In order to study the velocity of the fluid meniscus within the structures, while the fluid flowed the time was registered. Since the dimensions of the structure are known the time was recorded whenever the liquid turned the channel's curve.

The behavior of both pumps (*slow* and *fast*) was studied separately. Figure 3.1 demonstrates the position and velocity profiles for both pumps.

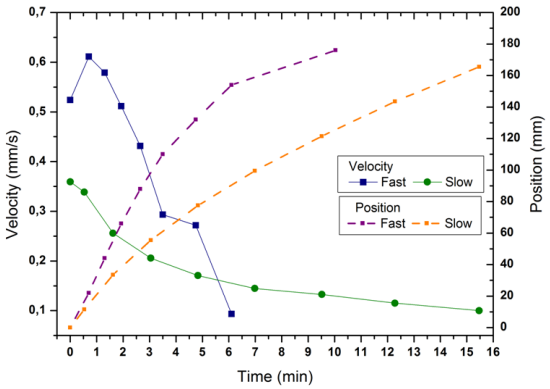

Figure 3.1 Velocity and position profiles for a dye experiment, in a slow and a fast pump

As expected, in a fast pump the velocity reaches higher values, illustrating the effect produced by the *passageways*. Considering that the *passageways* behave like valves that keep the liquid trapped and only allow it to flow when the fluid front reaches those spots (as illustrated in Figure 3.2).

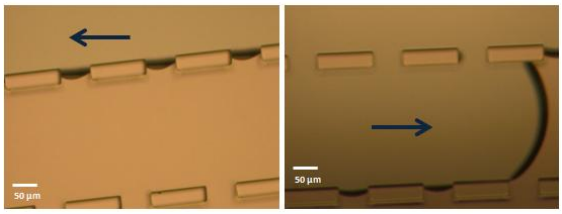

Figure 3.2 Microscopic view of a fast pump before (left) and after (right) the passage of the dye's fluid front (Olympus20x)

3.1.2 Surface treatment

The following point of interest has to do with the effect of surface treatment. As mentioned before, all the glass slides used to seal the structures were subjected to a UV/Ozone treatment. In several trials, the glass slides were treated, the structure sealed and stored. The exact time between the treatment and the experiment was not controlled, however it was at least 2h.

Therefore the hypothesis that the period of time between the glass treatment and the beginning of the experiment influenced the fluid behavior emerged. With the purpose of understanding this phenomenon various periods of time between treatment and experiment were tested, including 30minutes and 1h (Figure 3.3).

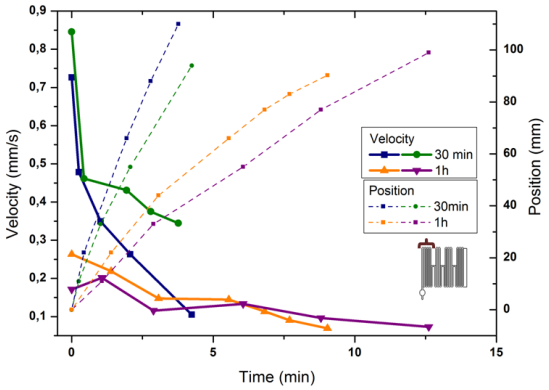

Figure 3.3 Velocity and position profiles of the fluid front, for the dye solution, in a slow pump, for experiments starting 30minutes and 1h after the UV/Ozone treatment of the glass slide

As can be observed in the graph, the influence of time after treatment can have significant changes in fluid flow behavior. For the same covered distance the structures of 30minutes show a time response of about half the ones that waited 1h, reaching fluid velocities of 0.7-0.9mm/s.

These results can be explained by th fact that after the treatment the tendency to adsorb contaminants increases.[18]These contaminants affect the contact angle of the liquids in the surface, and consequently its hydrophilicity.[28] The longer the time before the experiment, the higher the probability of accumulation of dust and particulate that affects the properties of the glass.

Considering a slow pump in the beginning of the structure, it is desired to have a reasonable value of velocity to assure the fluid flow through all the length. Therefore, if it takes too long to fill the first pump it will be difficult to guarantee that there will be enough driving force to pull all the solutions.

Taking these results into account for the following experiments the waiting time chosen was 30minutes.

3.1.3 Pump sequence

It is still important to understand the effect in fluid flow of placing different pumps in sequence. According to the following graphic (Figure 3.4) the blue and the orange regions correspond to the *slow* and *fast* pump, respectively, for two experiments.

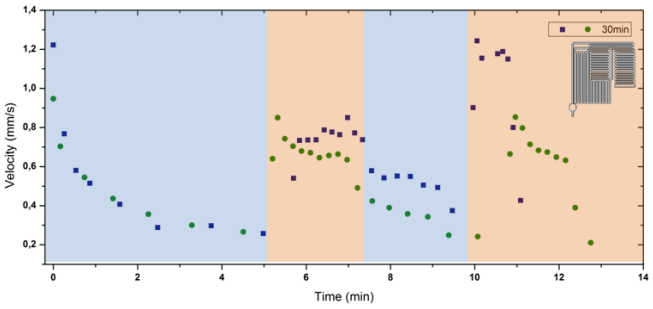

Figure 3.4 Velocity profile of the fluid front, for the dye solution, in the structure illustrated, for experiments starting 30minutes after the UV/Ozone treatment of the glass slide

As the fluid starts to flow through *slow1* velocity decreases, lasting about 5 minutes. Once the fluid front reaches *fast1* the fluid speed increases. As the fast pump gets filled the speed tends to decrease, however the variation is smaller than in the case of a *slow* pump. When reaching *slow2* the velocity keeps decreasing, now in a more pronounced way. At last the front gets to the final pump and once again there's a boost in speed. With the accumulation of resistance, in *fast2* the speed decreases until the fluid reaches the end of the microfluidic structure.

The comparison of the behavior of this structure with a similar one in literature[21] reveals that by sequentially placing different pumps is possible to simulate the necessary velocities for diverse assay steps.

Another important concept in microfluidics is flow rate. Flow rate corresponds to the volume of a certain fluid that flows through a surface in a certain period of time, can be approximated to the product of the flow velocity with the cross-sectional area of the channel (300µm width x 50µm height). While studying flow rate we are also including the geometry of the structure in which the assays are performed. Besides, the flow rate can give information about the volume of solutions necessary to fill each pump, according with the flowing time.

3.1.4 The importance of PBS

PBS is a saline buffer used frequently in dilutions. Since the preparation of the solutions for the immunoassays was done with PBS, this solution was chosen to study the response of the capillary system to a more viscous fluid. It was verified that for PBS experiments, starting 30minutes after treatment, the experimental time to fill the structure was larger than for the dye. Therefore, and taking into account that the solutions used in the assay are diluted in PBS, the following experiments were changed for a waiting time of 5 minutes.

Besides PBS, BSA was also tested. As Figure 3.5 shows the flow rates for these solutions are completely different. Taking into consideration the low flow rates for BSA and the adequate PBS response, the hypothesis of placing a small volume of PBS before the insertion of BSA came up. The volume of PBS introduced was 0.5µL, as the graph demonstrates is the enough amount to give the increment in terms of flow rate and it doesn't fill excessively the pumps intended for other solutions.

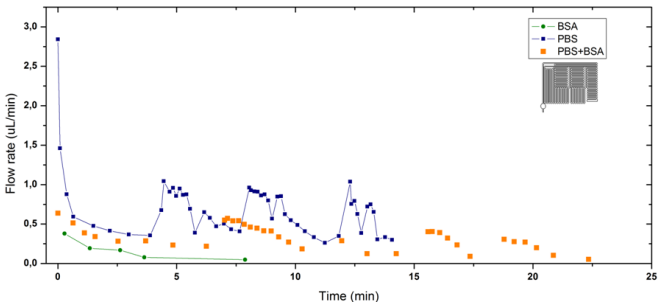

Figure 3.5 Comparison of flow rate, in the structure illustrated, for PBS, BSA and BSA with PBS experiments starting 5minutes after the UV/Ozone treatment of the glass slide

Taking these results into account, the best conditions to the realization of the OTA immunoassay were defined. Summing up, to perform an immunoassay in the proposed capillary system, it's fundamental to start the experiments between 5 and 10minutes after the glass treatment. As well it is necessary to insert 0.5µL of PBS before the introduction of BSA.

3.2 OTA immunoassay

After all the preparation of the capillary chips and of the solutions, everything is ready for the capillary icELISA. As described before the OTA immunoassay consisted in a step of spotting the OTA-BSA in the reaction chamber region, in the PDMS structure. Then and after evaporation the PDMS was sealed with the treated glass slide. Figure 3.6 shows a microscopic view of the spot after it dried and the structure sealed. The sketch of the reaction chamber indicates the orientation of the pictures. The decision of spotting the conjugate OTA-BSA instead of flowing it along with the other solutions was made, due to the existence of a spatially defined region for signal reading.

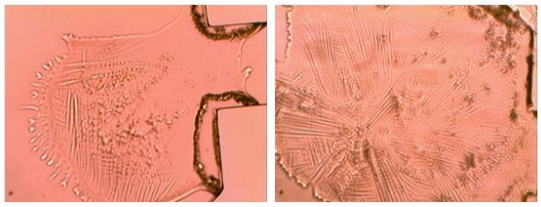

Figure 3.6 Microscopic view of the spotted OTA-BSA in the reaction chamber (AmScope 10x)

The flow rates and filling times associated with the icELISA protocol performed are summarized in Table 1. The general assay time is around 25 to 30minutes, depending not only on the capillary system, but also in the time spent in inserting manually the solutions into the inlet.

Table 1 Sequential steps of the capillary icELISA protocol

Immunoassay step	Filling time (min)	Average velocity (mm/s)	Flow rate (µL/min)	Volume (µL)
Blocking (BSA)	8	0,34	0,306	2
Washing (PBS)	3.5	0,53	0,477	1.2
Target antibody (anti-OTA HRP)	7	0,29	0,261	1.5
Washing (PBS)	3	0,42	0,378	1.2
HRP substrate (TMB)	5 3	0,18	0,162	3

The objective of the immunoassay tests in the capillary system was to investigate the ability to detect various concentrations of OTA. Particularly concentrations of 2ng/mL that correspond to the regulatory limit of OTA for wine.[20] The detection is possible through colorimetry. Therefore, in order to analyze the results several images obtained from an optical microscope and a cell phone camera are studied. (Figure 3.7)

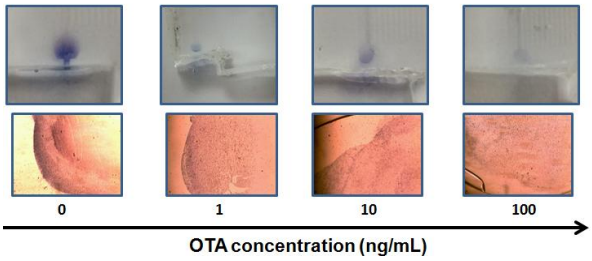

Figure 3.7 Comparison of colorimetric detection results, of several OTA concentrations prepared in buffer, in a cell phone camera (8.0MP) and in an optical microscope (Amscope 10x)

One way of doing a quantitative colorimetric measurement is by using a using a light source in the visible range and measure absorbance. In this case, the sample is excited by a light source of intensity I_0, and the amount of light that it is transmitted I is measured. Since the interest is to quantify the color produced during the reaction of the immunoassay species, I is obtained in the colored region, corresponding to the area where the OTA-BSA was spotted, and I_0 outside the spot region, as a reference.[26]

After this analysis the absorbance results were obtained (Figure 3.8). According to these results, the increase in OTA concentration leads to a decrease of signal, namely in absorbance. This can be explained by the fact that for a OTA concentration of 0ng/mL, when the solution of anti-OTA HRP is introduced in the system, all the antibodies are free to bind to the OTA-BSA conjugates immobilized in the PDMS structure. Whereas in a case where in the anti-OTA HRP solution is added a certain concentration of OTA, the antibodies will have the tendency to bind to the free OTA in solution. This way, when inserting this combination in the capillary system, the amount of free anti-OTA HRP able to bind to the immobilized antigens is smaller. Resulting

in a decrease in signal detected. Consequently, since the competition increases, the higher OTA concentration mixed with the anti-OTA HRP the less signal is detected.[19]

So, as expected the results show a decrease in colorimetry for an increase in OTA concentration. Since the signal decreases, and the colors are less intense the ratio between the transmitted and the emitted light increases. Therefore the transmittance of the system is enhanced. Consequently the absorbance level tends to be smaller.

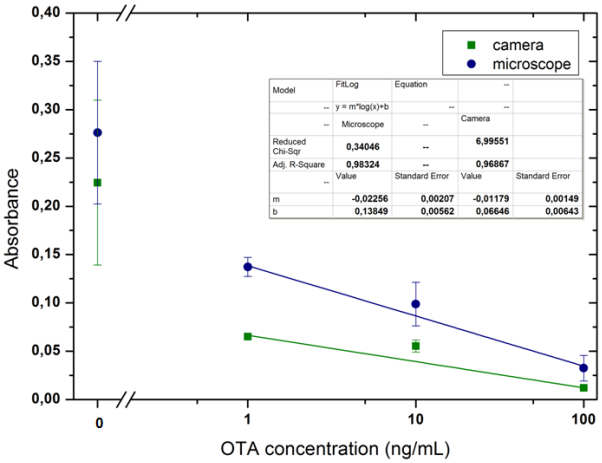

Figure 3.8 Comparison of the colorimetric detection, of several OTA concentrations prepared in buffer, for optical microscopy (Amscope 10x) and cell phone camera (8.0MP). The error bars (standard deviation) of the camera data were obtained with 3 samples per concentration value

One of the main interests on working with a colorimetric detection was to study the future possibility of importing the data with a cell phone camera. The reaction chamber format and dimensions are explained by this interest.

In order to study the quality of the acquired images of both cameras the absorbance was calculated and compared Figure 3.8. The differences are not drastic, however the decrease in absorbance depicted in the images obtained by the cell phone camera (8.0MP) is in concordance with the lack of resolution of the acquired photos. Not being able to perfectly define the reaction camber structure nor the colored spotted area. Therefore, to consider this acquisition method in the future, more work should be done in order to avoid loss of information.

These experiments showed that the capillary system is sensitive enough to allow the detection of OTA concentration within the regulatory limits.[20]

4 CONCLUSIONS

The main claims of this project are not only the development of a capillary chip capable of performing a multi-step immunoassay, but also the recognition of the critical points for its use. In capillary microfluidic devices several conditions, like chip characteristics, surface properties, contaminations are known to influence the chip behavior.

Considering the chip properties, the surface treatment can be considered one of the main discoveries associated with this work. The previous knowledge on surface properties like surface tension and contact angle was important as a starting point. Thus, PDMS is known for having a larger contact angle and therefore for its hydrophobicity. In contrast, glass is described in the literature as being hydrophilic. This information, led to the hypothesis of cleaning and treating glass in order to remove contaminants. However, after treatment it was noticed that not only glass gets cleaned but also there is an increase in its hydrophilic characteristics. The improvement in hydrophilicity is important, because induces a decrease in contact angle that in turn increases capillary pressure and flow rate.

Still it was also important to understand that these properties are dependent on the factor time, especially when considering a PoC application. The results demonstrate that for periods of time superior to 30minutes the flow rates reach low values. However when starting the experiments about 5minutes after the glass treatment and the sealing, the fluid front reaches the outlet in a shorter period of time. About this circumstance it also important to mention the influence of fluid viscosity. For a fluid with a higher coefficient of viscosity, the hydraulic resistance to fluid motion is higher and consequently the flow rate decreases.

In terms of the capillary structure used for the immunoassays, the sequence of pumps used was shown to be efficient in introducing the

right fluxes for the different steps that composed the assay.

Addressing the main conclusion of this project, it was shown that it is possible to customize a capillary microfluidic system to a specific application. In the perspective of PoC devices a capillary system can be very relevant, since it performs without the need of external equipments improving portability of the system. Besides, a short time analysis was provided (25-30min) only requiring the user intervention in loading the sequential solutions in the inlet.

BIBLIOGRAPHY

[1] S. Haeberle and R. Zengerle, “Microfluidic platforms for lab-on-a-chip applications,” *Lab Chip*, vol. 7, no. 9, p. 1094, 2007.

[2] MarketsandMarkets, “Microfluidics Market by Application, Material, Diagnostic & End User - 2020,” 2015.

[3] A. K. Yetisen and L. R. Volpatti, “Patent protection and licensing in microfluidics,” *Lab Chip*, vol. 14, no. 13, p. 2217, 2014.

[4] P. Novo, F. Volpetti, V. Chu, and J. P. Conde, “Control of sequential fluid delivery in a fully autonomous capillary microfluidic device.,” *Lab Chip*, vol. 13, no. 4, pp. 641–5, 2013.

[5] L. Gervais and E. Delamarche, “Toward one-step point-of-care immunodiagnostics using capillary-driven microfluidics and PDMS substrates.,” *Lab Chip*, vol. 9, no. 23, pp. 3330–3337, 2009.

[6] L. Gervais, M. Hitzbleck, and E. Delamarche, “Capillary-driven multiparametric microfluidic chips for one-step immunoassays,” *Biosens. Bioelectron.*, vol. 27, no. 1, pp. 64–70, 2011.

[7] C. C. Lin, J. H. Wang, H. W. Wu, and G. Bin Lee, “Microfluidic Immunoassays,” *JALA - J. Assoc. Lab. Autom.*, vol. 15, no. 3, pp. 253–274, 2010.

[8] D. J. Beebe, G. a Mensing, and G. M. Walker, “Physics and applications of microfluidics in biology.,” *Annu. Rev. Biomed. Eng.*, vol. 4, pp. 261–286, 2002.

[9] G. Bracco and B. Holst, *Surface science techniques*, vol. 51, no. 1. 2013.

[10] D. Juncker, “Capillary Microfluidic Systems for Bio / Chemistry,” 2002.

[11] H. Bruus, “Theoretical microfluidics,” *Physics (College. Park. Md).*, vol. 18, no. 33235, p. 363, 2008.

[12] W. van der Wijngaart, “Capillary pumps with constant flow rate,” *Microfluid. Nanofluidics*, pp. 1–9, 2014.

[13] B. J. Kirby, *Micro-and Nanoscale Fluid Mechanics: Transport in Microfluidic Devices*. Cambridge University Press, 2010.

[14] M. Zimmermann, H. Schmid, P. Hunziker, and E. Delamarche, “Capillary pumps for autonomous capillary systems,” *Lab Chip*, vol. 7, no. 1, pp. 119–125, Dec. 2007.

[15] A. Oláh, H. Hillborg, and G. J. Vancso, “Hydrophobic recovery of UV/ozone treated poly(dimethylsiloxane): Adhesion studies by contact mechanics and mechanism of surface modification,” *Appl. Surf. Sci.*, vol. 239, no. 3–4, pp. 410–423, 2005.

[16] P. N. Nge, C. I. Rogers, and A. T. Woolley, “Advances in Micro fl uidic Materials , Functions , Integration , and Applications,” 2013.

[17] G. Li, Y. Luo, Q. Chen, and J. Zhao, “a Capillary-Pressure-Based Air Pump for Nanoliter Liquid Handling in Microfluidic Devices,” *15th Int. Conf. Miniturized Syst. Chem. life Sci.*, pp. 918–920, 2011.

[18] W. R. Birch, “Cleaning Glass Surfaces,” in *Sol-Gel Technologies for Glass Producers and Users*, Springer Science & Business Media, 2004, pp. 30–35.

[19] R. R. G. Soares, P. Novo, a. M. Azevedo, P. Fernandes, M. R. Aires-Barros, V. Chu, and J. P. Conde, “On-chip sample preparation and analyte quantification using a microfluidic aqueous two-phase extraction coupled with an immunoassay,” *Lab Chip*, vol. 14, no. 21, pp. 4284–4294, 2014.

[20] European Commision, “Commission Regulation (EC) No 1881/2006, Setting maximum levels for certain contaminants in foodstuffs,” *Off. J. Eur. Union*, vol. 2006, no. 1881, pp. 5–24, 2006.

[21] P. Novo, “Advanced optical lab-on-chips for point-of-care applications,” 2014.

[22] U. H. V Ii, “Chapter II Process equipment and experimental techniques,” *Film*, pp. 19–53, 2000.

[23] MicroChem, “NANO ™ ANO ™ SU-8 Negative Tone Photoresist Formulations 50-100.”

[24] Elveflow, “SU-8 mold lithography,” 2015. [Online]. Available: http://www.elveflow.com/microfluidic-tutorials/soft-lithography-reviews-and-tutorials/introduction-in-soft-lithography/su-8-mold-lithography/. [Accessed: 22-Aug-2015].

[25] J. Landers, *Handbook of Capillary and Microchip Electrophoresis and Associated Microtechniques*. 2008.

[26] D. Li, *Encyclopedia of microfluidics and nanofluidics*, vol. 1. 2008.

[27] G. Cumming, F. Fidler, and D. L. Vaux, “Error bars in experimental biology.,” *J. Cell Biol.*, vol. 177, no. 1, pp. 7–11, Apr. 2007.

[28] Z. Li, Y. Wang, A. Kozbial, G. Shenoy, F. Zhou, R. McGinley, P. Ireland, B. Morganstein, A. Kunkel, S. P. Surwade, L. Li, and H. Liu, “Effect of airborne contaminants on the wettability of supported graphene and graphite.,” *Nat. Mater.*, vol. 12, no. 10, pp. 925–31, Oct. 2013.